Astronomy & Astrophysics manuscript no. TSWLatexianTemp_000005
May 19, 2023
©ESO 2023

α Cir - a benchmark roAp star

T. Kallinger[1], W. W. Weiss[1], and R. Kuschnig[2]

[1] Department of Astrophysics, University of Vienna, Türkenschanzstrasse 17, 1180 Vienna, Austria
[2] Institute of Physics, University of Graz, 8020 Graz, Austria

Received / Accepted

ABSTRACT

Context. α Cir is the brightest chemically peculiar magnetic (mCP) star, which is also pulsating. Even though mCP stars are in the research focus for decades, there are still unsolved and controversial issues concerning their structure and evolution. Precise photometric and spectroscopic data are needed, preferably with a long time base, to investigate also evolutionary aspects. This is closely fulfilled by the present investigation of α Cir: space-based high precision photometry with high time resolution, covering 20+ years and supplemented by high resolution spectroscopy from ground.
Aims. Discussion of the published controversial rotation periods and determination of the actual value. Processing the complex pulsation frequency spectrum, with implications for modelling the structure of α Cir.
Methods. An automated Bayesian algorithm was developed to consistently search for periodic signals in the WIRE, SMEI, TESS, and BRITE space photometric data sets, complemented by radial velocity data from HARPS.
Results. New observations in 2021 from TESS and BRITE indicate the detection of α Cir as a triple system. The rotation period of α Cir$_A$ is determined to 4.479290 ± 0.000002 d. The TESS data show a rich frequency spectrum including three $l = 0$, six $l = 1$, two $l = 2$ and one $l = 3$ modes, of which five are clearly rotationally split. The dipol modes show significant curvature in the echelle diagram, probably due to the strong magnetic field of α Cir.
Conclusions. α Cir continues to be a cornerstone of mCP stars. Confirmation of the triple system needs additional space photometry and/or high-resolution spectroscopy to increase the time base. These data are also needed to improve the quality of the pulsation frequency spectrum and to investigate evolutionary effects. Detailed seismic modelling, considering the effects of a magnetic field on pulsation is required, but is beyond the scope of the present paper.

Key words. stars: late-type - stars: oscillations - stars: fundamental parameters - stars: interior - stars: multiple systems

1. Introduction

α Cir is a prominent member of the rapidly oscillating chemically peculiar (roAp) stars, which formally was established by Kurtz (1982). The potential of non-radial and multi-mode pulsation for studying the structure and evolutionary status of stars all over the HRD became evident in these days and asteroseismology was established as a very powerful research tool (e.g. Gough 1985). The limitations of ground based observations, however, are serious (day-night cycles, weather gaps, seasons) and soon the potential of space observations was recognised (Aerts 2021).

Asteroseismic observations of α Cir span more then 40 years and cover photometry from ground (e.g. Kurtz et al. 1981; Schneider & Weiss 1983; Weiss & Schneider 1984) and space (e.g. Bruntt et al. 2009; Weiss et al. 2016, 2020), as well as spectroscopy (e.g. Schneider & Weiss 1989; Ryabchikova et al. 2007). This material makes α Cir a treasure trove for studying roAp stars, as is illustrated also by recent surface mapping of α Cir, which indicates at least three spots with probably different chemical composition on its surface (Weiss et al. 2020).

In the following we investigate photometric time series from four different space mission and spectroscopy from ground covering more than 20 years of observations. Small but statistically significant long-term changes of the main pulsation frequency indicate a close low-mass companion of α Cir, which – if proven – makes it the first discovery of a secondary star only from the pulsation signal of the primary. Furthermore we present the so far richest frequency spectrum of any roAp star and find no evidence yet for evolutionary changes of the stellar rotation period on a sub-ppm level.

Send offprint requests to: thomas.kallinger@univie.ac.at

2. Data

2.1. WIRE

Soon after launch in March 1999 of the Wide Field Infrared Explorer (WIRE) the hydrogen cryogen boiled off due to a technical defect terminating the primary science mission. But the onboard star tracker with 52mm aperture remained functional and could be used for photometry till 2006 (e.g. Buzasi 2002), when communication with the satellite failed.

α Cir was observed for a total of 84 days with the WIRE star-tracker in September 2000, February 2005, and February and July 2006. Bruntt et al. (2009) were the first to process the raw data and analyse the inherent pulsation signal, followed by Weiss et al. (2020) who used the same data primarily for spot modelling. Here we re-assess the Bruntt et al. (2009) data, but combine the February and July data sets of 2006 for an improved frequency resolution (see Tab. 1).

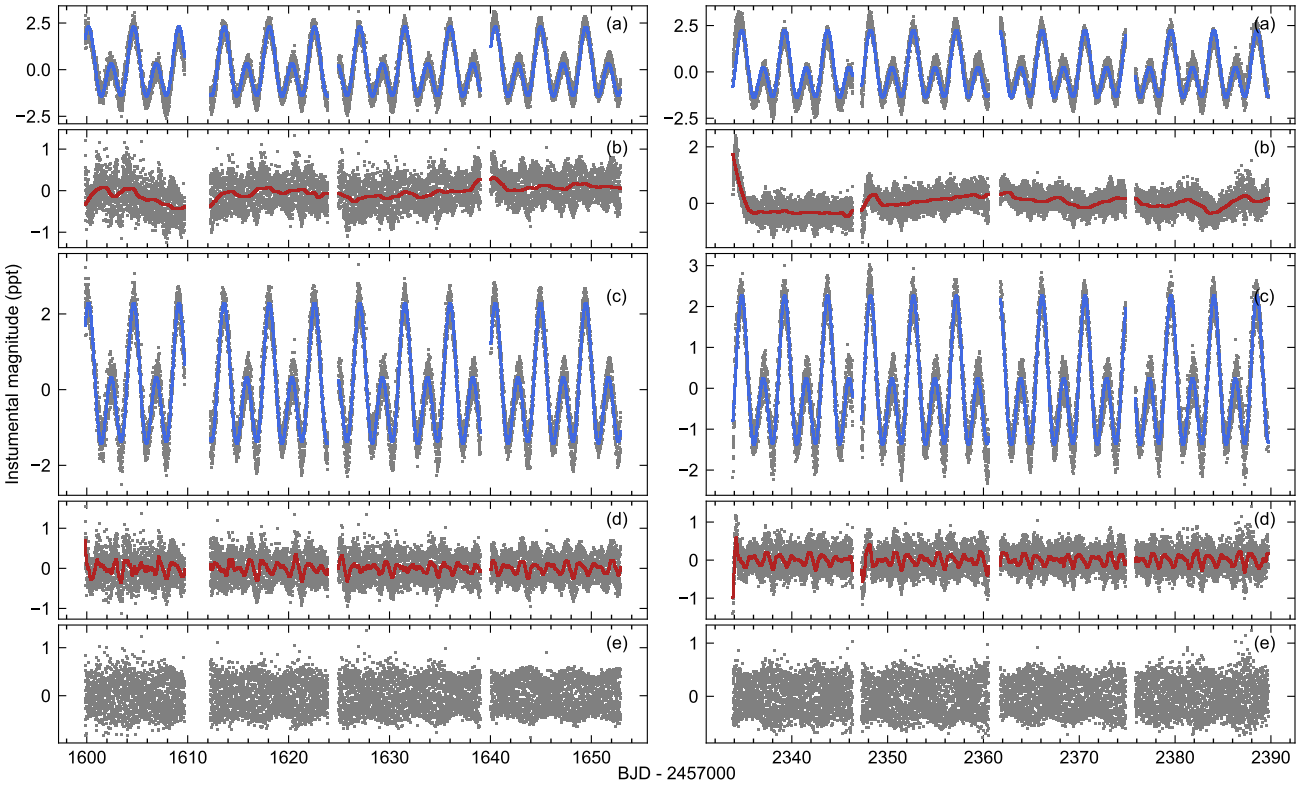

Fig. 1. TESS 2019 (left) and 2021 (right) SPOC light curves. *Panels (a)*: Double harmonic fit (blue lines) to the original SPOC data (grey dots). *Panels (b)*: Original (grey dots) and heavily smoothed (red lines) residuals to the double harmonic fit of panel (a). *Panels (c)*: Original SPOC data corrected for the smoothed residuals from panel (b) (grey dots – these data are used for the rotation analysis) along with a double harmonic fit (blue lines). *Panels (d)*: Original (grey dots) and heavily smoothed residuals (red lines) from panel (c). *Panels (e)*: Residuals from panels (d). These data are used for the pulsation analysis.

2.2. SMEI

The Solar Mass Ejection Imager (SMEI) is an instrument on board the Coriolis satellite. The three CCD cameras of the instrument observe the whole sky in order to detect disturbances in the solar wind. Besides this primary science goal, the data were used to detect stellar pulsations in bright stars (e.g., Jackson et al. 2004). α Cir was observed by SMEI for almost 2900 days between February 2003 and December 2010 (see Tab. 1). Raw SMEI data suffer from very strong instrumental effects so that data post-processing is a rather complicated procedure. Weiss et al. (2020) provides more details on the procedure.

2.3. TESS

α Cir has been observed with TESS (Ricker et al. 2015) from April to June 2019 for about 54 d as target in sector 11 and 12 and for additional 54 d from April to June 2021 in sector 38 and 39. For the present study, we use the photometric time series provided by the TESS Science Processing Operations Center pipeline (Jenkins et al. 2016, SPOC) and accessible via the Mikulski Archive for Space Telescopes (MAST) at the Space Telescope Science Institute. The data are shown in Fig. 1.

To minimise instrumental long-term trends in the time series, we fit amplitudes (a_n) and phases (ϕ_n) of a double harmonic function to the original time series according to:

$$f(t) = a_1 \cos\left(2\pi\left[\frac{t}{P} + \phi_1\right]\right) + a_2 \cos\left(2\pi\left[\frac{2t}{P} + \phi_2\right]\right), \quad (1)$$

with a fixed period $P = 4.47928$ d. In a next step a 2nd order Savitzky-Golay filter, with a window length of about 2.8 d, is applied to the residual data. The resulting trend (see red lines in Fig. 1b) is then subtracted from the original data (Fig. 1c) giving the final time series used for the rotation analysis.

For the pulsation analysis we apply Eq. 1 again on the corrected data, but now use a shorter window length of about 6.7 h for smoothing. The final 2019 and 2021 light curves are shown in Fig. 1e and have a point-to-point scatter[1] of ~0.51 and ~0.49 ppt, respectively, which translates to a high-frequency Fourier noise of about 1.43 and 1.38 ppm.

2.4. BRITE

α Cir was observed in 2014 for a total of 145 d during the commissioning phase of BRITE-Constellation and the results were analyzed by Weiss et al. (2016). Subsequent observations of the star were carried out in 2016 for 163 d by three from the five operational BRITE satellites, forming the basis for the investigations presented by Weiss et al. (2020). The photometric measurements and data reduction are described in the mentioned study.

In addition, α Cir was observed by BRITE-Toronto in the field 62-CruCar-III-2021, from March 21, 2021, to August 23, 2021, for a total of 136 d. The satellite collected 10 to 30 measurements per satellite orbit, with a typical sampling rate of 20 s and an exposure time of 1 s. The raw images were processed using the pipeline described by Popowicz et al. (2017), which

[1] square root of the mean squared difference of consecutive data points

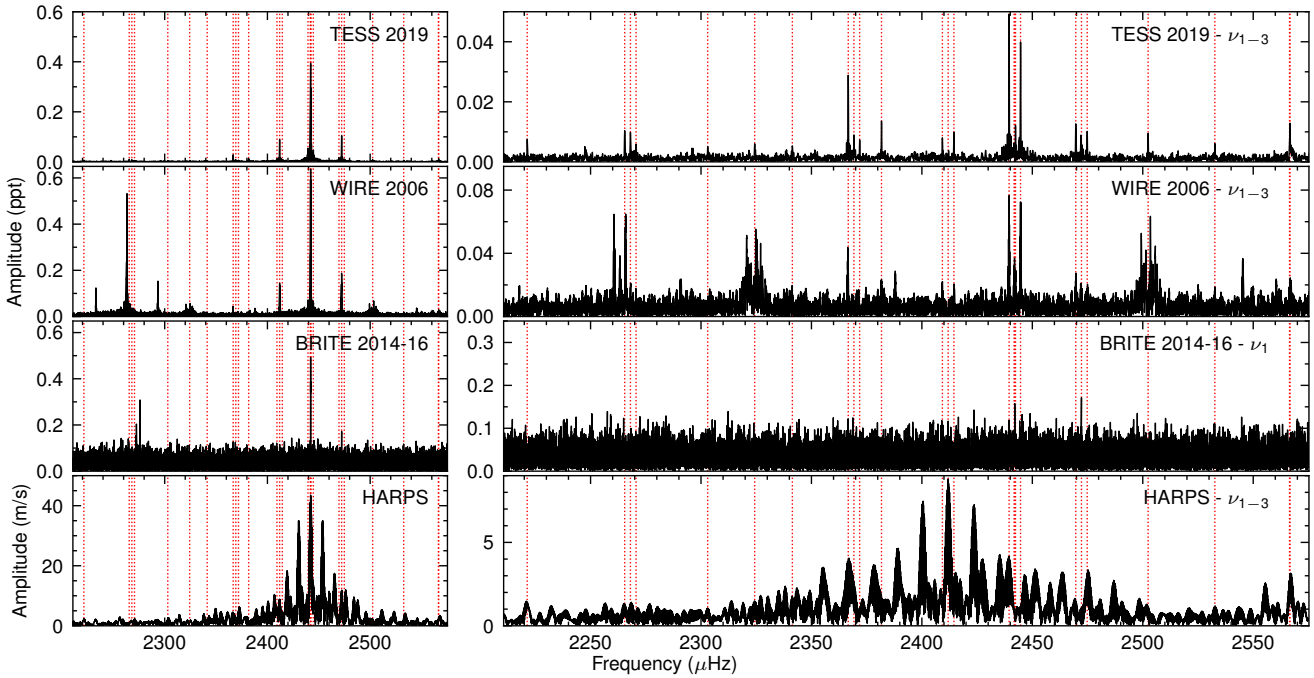

Fig. 2. Fourier amplitude spetra of the TESS 2019, WIRE 2006, combined BRITE 2014-16 light curves, and the HARPS radial velocities with the significant TESS frequencies overlaid as vertical red dotted lines. The original spectra are shown in the left panels, whereas right panels give the spectra after prewitheing the one to three most significant frequencies.

Table 1. Photometry of α Cir from space and spectroscopy from ground. Given are the approximate effective wavelengths and band widths of the different photometers in nm, the duration $T_{\rm obs}$, the number of data points, and the start and end date of the observations.

Season	$T_{\rm obs}$ [d]	Number of data points	Start [yyyy-mm-dd]	End
Photometry:				
		WIRE ($\lambda \simeq 600 \pm 190$)		
2000	42.1	26359	2000-08-18	2000-09-29
2005	8.3	10857	2005-02-16	2005-02-25
2006†	171.2	56673	2006-02-10	2006-07-31
		SMEI ($\lambda \simeq 630 \pm 300$)		
2003/10	2885	23703	2003-02-03	2010-12-30
		TESS ($\lambda \simeq 800 \pm 200$)		
2019	53.0	34425	2019-04-22	2019-06-19
2021	51.9	37706	2021-04-28	2021-06-24
		BRITE ($\lambda \simeq 605 \pm 70$)		
2014	145.3	64037	2014-03-03	2014-08-08
2016	163.7	31257	2016-02-04	2016-07-22
2021	136.4	46367	2021-03-21	2021-08-23
Spectroscopy:				
		HARPS (echelle spectra: λ 378 − 691)		
2008††	60.2	4869	2008-02-20	2008-04-20

Notes. $^{(\dagger)}$ The WIRE 2006 data have a gap from March 15 to July 7 (114 days).
$^{(\dagger\dagger)}$ HARPS data have a gap from February 23 to April 16 (52 days).

accounts for the technical issues that are typical for BRITE photometry, like hot pixels (Pablo et al. 2016). The extracted photometry[2] still includes systematic instrumental effects due to CCD temperature drifts and the position of the star's point spread function in the raster. These effects were minimized using the same approach as for TESS photometry, described in section 2.3. α Cir was also observed in 2018 with one of the BRITE satellites, but since the resulting time series is significantly shorter (~65 d) and noisier than the other BRITE data sets, it does not contribute to the current analysis, which is why we decided to ignore it for the time being.

2.5. HARPS

Even though there are plenty of high-resolution spectroscopic observations available for α Cir, they are typically not suited for a detailed frequency analysis due to the usually short time base of hours up to a few days of the spectra. An exception are the more than 4800 echelle-spectra obtained during nine nights in February and April 2008 with the High Accuracy Radial velocity Planet Searcher (HARPS) spectrograph of the European Southern Observatory's 3.6-m telescope at La Silla. The campaign was presented by Mkrtichian & Hatzes (2013), but no asteroseismic analysis has yet been published. For our frequency analysis we use radial velocity measurements from the HARPS RV database (Trifonov et al. 2020).

3. Pulsation

To extract the oscillation parameters from the light curves, we apply an updated version[3] of the probabilistic approach presented by Kallinger & Weiss (2017). The automated Bayesian algorithm was originally developed to handle multiple close frequencies within the formal frequency resolution (Kallinger et al.

[2] taken from the BRITE public data archive
[3] autoDFT on Github

Table 2. Significant pulsation frequencies from TESS 2019 and 2021 observations, sorted by their appearance in the 2019 prewhitening sequence. Frequencies and amplitudes are given in μHz and ppm, respectively, and the errors in units of the last digit. The parameter p gives the probability that a frequency is statistically significant compared to noise. The last column lists the relative change in ppm of the pulsation frequencies from 2019 to 2021.

	TESS 2019: t_0 = 2458583				TESS 2021: t_0 = 2459318				
	$\nu\,(\mu Hz)$	$\delta\nu_{rot}$	a (ppm)	p	$\nu\,(\mu Hz)$	$\delta\nu_{rot}$	a (ppm)	p	$\frac{\nu_{2021}-\nu_{2019}}{\nu_{2019}}$
ν_1	2442.0722±05	2.588±3	395±1	1.0	2442.0175±07	2.581±04	378±2	1.0	-22.3±0.4
ν_{1-}	2439.4854±34		49±1	1.0	2439.4367±61		44±3	1.0	
ν_{1+}	2444.6609±39		40±1	1.0	2444.5994±65		41±2	1.0	
ν_2	2472.2498±15	2.581±10	105±1	1.0	2472.1812±32	2.599±29	90±3	1.0	-27.7±1.4
ν_{2-}	2469.662±14		13±1	1.0	2469.593±43		8±3	0.70	
ν_{2+}	2474.843±14		10±1	1.0	2474.791±38		9±3	0.84	
ν_3	2411.8964±18	2.608±14	90±1	1.0	2411.8522±37		76±2	1.0	-18.3±1.7
ν_{3-}	2409.284±22		8±1	1.0					
ν_{3+}	2414.500±16		10±1	1.0					
ν_4	2566.658±14		13±1	1.0					
ν_5	2381.718±12		13±1	1.0	2381.682±30		10±3	0.95	-15±14
	2472.014±19		10±1	1.0					
ν_6	2268.041±19	2.574±17	9±1	1.0	2268.016±23	2.597±36	11±2	0.99	-11±13
ν_{6-}	2265.456±16		10±1	1.0	2265.419±28		10±3	0.95	
ν_{6+}	2270.604±31		5±1	0.96					
ν_7	2369.220±18	2.576±13	9±1	1.0					
ν_{7-}	2366.6590±55		29±1	1.0	2366.602±11		26±3	1.0	
ν_{7+}	2371.812±27		6±1	0.99					
ν_8	2502.431±16		9±1	1.0	2502.368±35		8±3	0.78	-25±15
	2442.387±22		9±1	1.0	2442.255±29		9±3	0.93	-54±15
ν_9	2221.316±29		7±1	1.0					
	2441.738±29		7±1	0.99	2441.811±12		21±2	1.0	30±13
ν_{10}	2324.312±31		6±1	0.98					
	2566.450±26		6±1	0.97	2566.404±59		8±3	0.92	-18±25
ν_{11}	2532.632±29		6±1	0.97					
ν_{12}	2341.357±44		5±1	0.91					
	2567.600±160		5±1	0.91					
average:		2.586±3				2.584±5			-21.8±0.5

2017) but it works with a mono-periodic signal (within one formal frequency resolution bin) as well. The software uses the Python version (Buchner 2016, UltraNest) of the nested sampling algorithm MultiNest (Feroz et al. 2009) to search for periodic signals in time series data and tests their statistical significance by comparison with no signal (i.e. only noise). A solution is considered real[4] (i.e. not due to noise) if its probability $p = z_{signal}/(z_{signal} + z_{noise}) \geq 0.91$, where z is the global evidence[5] delivered by UltraNest. The approach has been extensively tested with artificial data (Kallinger & Weiss 2017) and the subsequent results have been randomly compared with those from Period04 (Lenz & Breger 2005). In all cases agreement was found within the uncertainties.

The dominant 6.8 min ($\approx$2442 μHz) pulsation period is known for more than 40 years and has frequently been studied (e.g. Kurtz & Balona 1984; Schneider & Weiss 1983, 1989) after its discovery (Kurtz 1982). Rotational split components with $\delta\nu_{rot} = 2.593 \pm 0.006\,\mu$Hz next to the dominant frequency were first detected by Kurtz et al. (1994), based on the combination of multiple ground-based observing runs and later on confirmed by (Bruntt et al. 2009) with WIRE data. However, the results of the two studies are inconsistent in a sense that frequencies found to be significant in one data set do not show up in the other and vice versa. Meanwhile, this ambiguity is settled thanks to the high-precision time series of TESS.

3.1. TESS

Obviously, the most significant time series in our set of space-based photometry are those from the TESS satellite. Observations of α Cir were first reported by Holdsworth et al. (2021) as part of a systematic search for roAp stars in the southern hemisphere with TESS, but include no detailed analysis and interpretation of the data.

Using the above described Bayesian approach, we identified 17 significant (i.e., $p \geq 0.91$) frequencies in the 2019 data (see Tab. 2), of which five modes (ν_1, ν_2, ν_3, ν_6, and ν_7) show a clear triplet structure with an average split frequency of $2.586 \pm 0.003\,\mu$Hz. Five more frequencies are very close ($\lesssim 0.3\,\mu$Hz) to frequencies with a significantly larger amplitude indicating some long-period ($\gtrsim$ 40 d) amplitude modulation, which we ignore for the sake of simplicity leaving a total of 12 independent pulsation frequencies. Figure 2 illustrates the original Fourier amplitude spectrum and the spectrum after

[4] According to the convention established by Jeffreys (1998), the evidence for or against one of two hypotheses is considered "substantial" for $p \gtrsim 0.75$, "strong" for $p \gtrsim 0.91$, and "very strong" for $p \gtrsim 0.97$.

[5] The global evidence is a normalised logarithmic probability describing how well the model fits the data with respect to the uncertainties, parameter ranges, and the complexity of the fitted model.

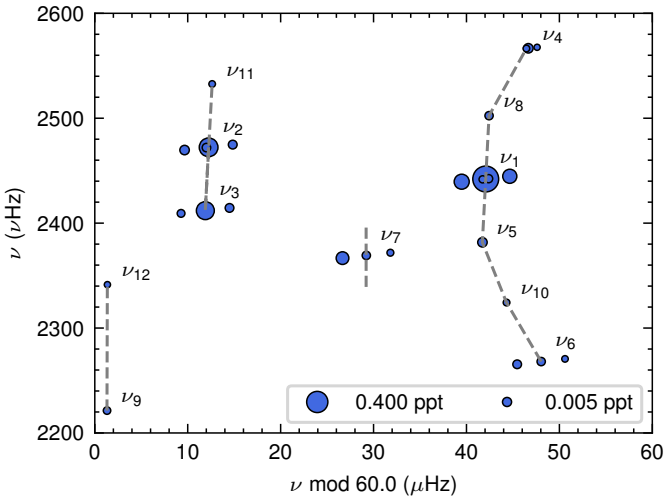

Fig. 3. Echelle diagram of the TESS 2019 frequencies with the symbol size indicating the mode amplitude and the annotation according to Tab. 2. Modes of presumably the same spherical degree are connected by dashed line segments.

prewhitening the first three frequencies. We note that all ten frequencies given by Holdsworth et al. (2021) are included in our list as well.

Figure 3 presents the 2019 TESS frequencies in an echelle diagram. It shows that the five rotationally split modes (ν_1, ν_2, ν_3, ν_6 and ν_7) are most likely of different spherical degree l. They form (together with the non-split modes) at least two mode sequences of consecutive radial overtones of the same spherical degree. It is remarkable that the best populated sequence around ν_1 is significantly curved even though high-radial order modes should rather follow a straight line in the echelle diagram (e.g. Tassoul 1980).

When analysing the 2021 TESS data set we could not reproduce the full set of frequencies from 2019. In fact, 12 of the 27 previously identified peaks are not significant in the new data even when lowering the probability threshold to 0.7. One might speculate that the photometric quality of the 2021 observations is not as good as for the 2019 data so that some low amplitude peaks remain unidentified due to an increased instrumental noise. However, it is the other way round. The photometric quality of the 2021 data is slightly better than that of the 2019 run, as is discussed in Sec.2.3. A closer look on the mode amplitudes actually shows that nearly all have systematically decreased by up to 10%, indicating that pulsation of α Cir has undergone some significant changes between 2019 and 2021. Even more interesting is the highly significant frequency decrease during the same observing period (see Tab.2, rightmost column).

3.2. BRITE

As we have slightly modified the data processing of the BRITE photometry for the present analysis compared to Weiss et al. (2020), we re-analysed the pulsation signal. An additional data set is now available, which makes a total of three (Tab. 1). Weiss et al. (2020) analysed the combined 2014 and 2016 BRITE data and found five significant frequencies. Here we are more interested in the temporal stability of the dominant frequency and therefore individually analyse the various data sets. In that sense, only ν_1 and ν_2 are statistically significant in the three BRITE data sets (Tab. 3).

3.3. WIRE

In their pulsation analysis, Weiss et al. (2020) focused on the 2006 data of WIRE. Here, we re-analyse all available WIRE data individually, where we only combine the February and July data sets of 2006 for an improved frequency resolution. While in the 2000 and 2005 data only ν_1 is significant, the 2006 time series shows six significant frequencies (see Tab. 3) that are all consistent with the TESS frequencies and the findings of Bruntt et al. (2009).

3.4. HARPS

Even though the HARPS radial velocity data suffer from 1 d^{-1} aliases (see Fig. 2), which are typical for ground-based observations, they show the richest pulsation frequency spectrum apart from the TESS data. We find 11 significant frequencies including an accurately defined triplet around ν_1. More interesting are the mode amplitudes, more specifically the amplitude ratios between the central and wing components of the determined triplets. For the photometric amplitudes of ν_1, ν_2, and ν_3, this ratio is in the order of 10:1. While the lower frequency wing component ν_{1-} follows this patter in the HARPS data, the amplitude of ν_{1+} is more than twice as high. We currently have no explanation for this discrepancy.

Another interesting phenomenon is the amplitude distribution in the ν_7 triplet. The amplitude of ν_{7-} in the TESS 2019 data is about three times as high as of the central component. This is kind of reproduced by the HARPS data, where we find the lower frequency component to have about twice the amplitude of the central one. This might be an indication that we miss-identified the modes and the triplet is actually a quintuplet with the two lower-frequency components being undetected. Future observations (especially the upcoming TESS observations) might help to solve this problem.

4. Binarity and pulsation

Two values of ν_1, derived from TESS 2019 and 2021 data, are presented in Tab. 2. Six values of ν_1 derived from BRITE and WIRE space photometry are listed in Tab. 3, together with one value derived from spectroscopy (HARPS). In addition, four values refering to published early ground based data are given also in this Table. Hence, a total of 13 ν_1-values are distributed over almost 40 years and range from 2441.9999 μHz (Kurtz et al. 1994) to 2442.0722 μHz (TESS 2019). These frequencies, with typical uncertainties of less than 5 nHz, are spread over an interval of about 70 nHz, which indicates that these variations are intrinsic and not due to noise.

The 13 measurements of ν_1 are shown in Fig. 4, which graph somehow reminds of the radial velocity curve of a single-lined spectroscopic binary. In fact, the orbital motion of a binary system modulates the stellar pulsation frequency due to the Doppler effect such that for a remote observer the frequencies will be shifted.

α Cir is known to be part of a visual binary system (e.g., Sinachopoulos 1989; Monier 2020) with a yet unknown but centuries-long orbital period. This known companion therefore cannot generate the observed modulation of ν_1, but a yet unknown companion could do so.

Table 3. Significant pulsation frequencies in the WIRE, BRITE, and HARPS observations derived in the present analysis and completed by literature values. Frequencies are given in μHz, amplitudes are in ppt for photometric data and m/s for HARPS. The parameter p gives the probability that a frequency is statistically significant compared to noise.

ν	$\delta\nu_{rot}$	a	p
BTr14: t_0 = 2456774			
ν_1 : 2442.058±0.006		517±45	1.0
ν_2 : 2472.235±0.010		221±45	1.0
BTr16: t_0 = 2457476			
ν_1 : 2442.060±0.004		634±37	1.0
ν_2 : 2472.221±0.008		174±38	0.99
BTr21: t_0 = 2459336			
ν_1 : 2442.031±0.004		583±49	1.0
ν_2 : 2472.208±0.011		212±52	0.98
WIRE 2000: t_0 = 2451751			
ν_1 : 2442.039±0.002		557±6	1.0
WIRE 2005: t_0 = 2453379			
ν_1 : 2442.059±0.014		657±13	1.0
WIRE 2006: t_0 = 2453751			
ν_1 : 2442.0548±0.0002	2.626±0.001	652±4	1.0
ν_{1-} : 2439.4694±0.0014		81±4	1.0
ν_{1+} : 2444.7223±0.0026		75±4	1.0
ν_2 : 2472.2260±0.0006		186±4	1.0
ν_3 : 2411.8815±0.0008		145±4	1.0
ν_{7-} : 2366.4734±0.0025		45±4	1.0
HARPS 2008: t_0 = 2454556			
ν_1 : 2442.0662±0.0001	2.5874±0.0007	43.4±0.1	1.0
ν_{1-} : 2439.4643±0.0013		4.1±0.1	1.0
ν_{1+} : 2444.6391±0.0005		10.4±0.1	1.0
ν_2 : 2472.2205±0.0005		10.7±0.1	1.0
ν_3 : 2411.9119±0.0006		8.8±0.1	1.0
ν_4 : 2466.9204±0.0019		3.2±0.1	1.0
ν_6 : 2268.49±0.10		1.2±0.1	1.0
ν_7 : 2369.3467±0.0022	2.6010±0.0026	2.4±0.1	1.0
ν_{7-} : 2366.7457±0.0013		4.1±0.1	1.0
ν_9 : 2221.03±0.10		1.2±0.1	1.0
ν_{12} : 2341.2952±0.0046		1.7±0.1	1.0
literature values			
Kurtz (1982): t_0 = 2444764			
ν_1 : 2442.027±0.033			
Kurtz & Balona (1984): t_0 = 2445174			
ν_1 : 2442.040±0.002	2.57±0.19	2100±80	
ν_{1-} : 2439.47±0.19		330±80	
Kurtz et al. (1994): t_0 = 2449111			
ν_1 : 2441.9999±0.0009	2.593±0.006	2548±17	
ν_{1-} : 2439.4034±0.0091		242±17	
ν_{1+} : 2444.5900±0.0076		294±17	
Baldry et al. (1998): t_0 = 2450142			
ν_1 : 2442.039±0.002		1740±70	

For a Keplerian orbit, the modulation of the intrinsic pulsation frequency γ can be computed for a given time t according to:

$$\nu = \gamma + K_\nu[\cos(\omega + \varphi_{(t,e,T,P)}) + e\cos\omega], \quad (2)$$

with the modulation amplitude K_ν, the longitude of the periastron ω, and the true anomaly φ, which depends on t, the eccentricity e, the periastron epoch T, and the orbital period P.

We again use UltraNest to fit Eq. 2 to the measurements of ν_1 and find a highly significant solution for an eccentric orbit with a period of 27.14 ± 0.16 yr. The full solution is listed in Tab. 4 and the corresponding fit and its uncertainties are shown in Fig. 4.

Table 4. Binary orbit solution.

γ	2442.05103 ± 0.00069 μHz
K_ν	0.053 ± 0.016 μHz
P	27.14 ± 0.16yr
T	1992.76 ± 0.22yr
e	0.868 ± 0.036
ω	2.18 ± 0.12rad
$f_{(m)}$	0.035 ± 0.033$M_\odot$

The relative frequency change translates into a radial velocity amplitude according to

$$K_{RV} = \frac{cK_\nu}{\gamma}, \quad (3)$$

which results in 6.5 ± 1.9 km/s for α Cir. We can now calculate the mass function,

$$f_{(m)} = \frac{(M_2 \sin i)^3}{(M_1 + M_2)^2} = \frac{PK_{RV}^3}{2\pi G}(1 - e^2)^{1.5}, \quad (4)$$

to 0.035 ± 0.033 $M_\odot$, where M_1 and M_2 are the mass of $\alpha\,\mathrm{Cir}_A$ and its companion, respectively. Using a primary mass of 1.7 ± 0.2 $M_\odot$(Bruntt et al. 2008) we can solve Eq. 4 for M_2 as a function of the systems inclination i. This is illustrated in Fig. 5, showing that the mass of the companion ranges from some tenth to a few solar masses, depending on the inclination of the binary system. The mass estimate can further be used to determine the orbital separation a of the two stars

$$a = \frac{PK_{RV}}{2\pi}(1 + \frac{M_1}{M_2}), \quad (5)$$

which is also given as a function of $\sin i$ in Fig. 5, showing that the system's size is comparable to our outer solar system[6].

In summary, we claim the detection of α Cir as a triple system, with the second companion orbiting $\alpha\,\mathrm{Cir}_A$ in an eccentric orbit every about 27 yr.

5. Rotation

The rotation period of α Cir has first been published by Kurtz et al. (1994) to P_{rot} = 4.4790 ± 0.0001 d. Using spot modelling based on WIRE and the early BRITE and TESS data, Weiss et al. (2020) improved P_{rot} to 4.47930 ± 0.00002 d .

The orbital motion of α Cir should in principle also affect the rotation period determined by an external observer, as is demonstrated in the previous section. But since P_{rot} is about 950 times longer than the main pulsation period, the resulting variation of the rotation period will be 950 times smaller than for the pulsation signal (see Eq. 3). We can thus expect such an effect to be on the order of ±0.00005 d (or ±4 s), which is comparable to the uncertainties of the so far best determined rotation period and much smaller than the error of P_{rot} when determined from the individual data sets. It is therefore inefficient to analyse the various data

[6] Note that at α Cir's distance of about 16.7 pc such a system has an apparent diameter of less then 0.05 milliarcseconds.

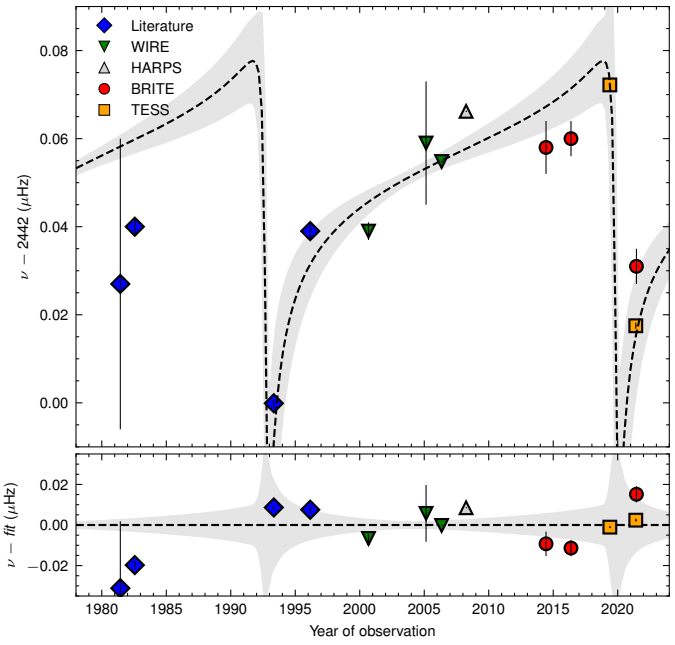

Fig. 4. Evolution of the main pulsation frequency ν_1 (top) with a binary orbit fit (dashed line) according to Tab. 4 and the residuals to the fit (bottom). The grey-shaded areas indicating the uncertainties.

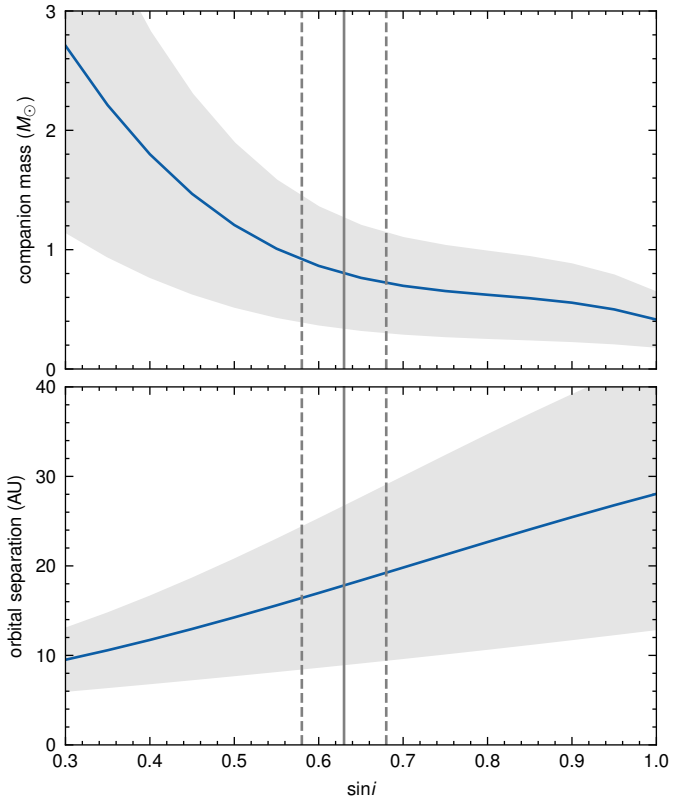

Fig. 5. Range of companion mass (top) and orbital separation (bottom) and their uncertainties (grey-shaded areas) for models as a function of the orbit inclination. The vertical lines indicate the inclination of the rotation axis of α Cir and its uncertainty.

sets individually with, e.g., classical frequency analyses, or even complex spot modelling.

A sensitive method to investigate the temporal stability of a periodic signal is based on a classical $O-C$ approach (e.g. Breger & Pamyatnykh 1998). With a time base of almost eight years, the SMEI data set provide a solid initial guess for P_{rot}. We thus fit Eq. 1 to the SMEI data, but unlike for data preparation (Sec. 2), we let P be a free parameter in the fit and determine it to 4.47908 ± 0.00009. In a next step we use this to phase fold the individual data sets and fit a double harmonic function (Eq. 1) with a fixed period to determine the phase of maximum light, ϕ_{max}. If the star's rotation period is constant and equal to the initial guess, ϕ_{max} would be the same for all data sets. If the initial guess slightly differs from the correct value, ϕ_{max} would linearly increase or decrease with time. If, however, the star's rotation period is varying, e.g. due to evolutionary changes of the stellar radius or due to changes of the star's angular momentum, ϕ_{max} would parabolically change.

In fact, Fig. 6 shows that ϕ_{max} increases with time and a parabolic fit $\phi_{max}(t) = d + kt + \beta t^2$, with $k = (1.05 \pm 0.01) \times 10^{-5}$ and $\beta = (-6 \pm 10) \times 10^{-11}$, shows that the increase is practically linear. The coefficient k of the linear term now allows us to correct the initial guess of the rotation frequency ($\nu_{rot} = 1/P_{rot}$) according to $\nu_{rot,cor} = \nu_{rot,initial} - k$, which gives a corrected rotation period of 4.479290 d. This values is then used to repeat the procedure. Now the fit gives $k = (6 \pm 10) \times 10^{-8}$ and the same β as before so that $\phi_{max}(t)$ is now constant within the uncertainties (see bottom panel of Fig. 6).

6. Discussion

The echelle diagram of the 2019 high-precision time series of TESS (Fig. 3) shows that the five rotationally split modes (ν_1, ν_2, ν_3, ν_6 and ν_7) are most likely of three different degrees l. Based on simulated amplitude modulations for an oblique pulsator model, Bruntt et al. (2009) argued that ν_1 is very likely an axisymmetric dipole mode ($l = 1, m = 0$). From this follows that, ν_4, ν_5, ν_6, ν_8, and ν_{10} are also dipole modes, ν_2, ν_3, ν_{11} are radial modes (see also Weiss et al. 2020), ν_9 and ν_{12} are $l = 2$ modes, and ν_7 is likely a $l = 3$ mode.

One might argue that radial modes are usually not rotationally split. A possible explanation for the claimed splitting is, however, that the significantly inhomogeneous surface of α Cir modulates the pulsation amplitudes with the rotation period, so that radial modes are also split in the Fourier domain. Another phenomenon, mentioned in Section3.1, is the significantly curved dipole mode sequence in Fig. 3, contradicting theory (e.g. Tassoul 1980) which claims that high-radial order modes follow a straight line. This anomaly could be a consequence of the observed modes being distorted (e.g. Cunha 2006) by the strong magnetic field of α Cir (e.g. Mathys 2017).

Another peculiarity of α Cir is a systematic decrease of nearly all pulsation mode amplitudes between 2019 and 2021 by up to 10% and the highly significant frequency decrease during the same observing period. For the high-amplitude modes we find on average a frequency shift of -21.8 ± 0.5 ppm. For ν_1 this shift is even -55 ± 8 nHz. But this trend is less obvious for the low-amplitude modes. Before the TESS and BRITE observations in 2021 became available we assumed that the change in ν_1 is the signature of stellar evolution. In fact, Fig. 4 shows a statistically significant, almost linear increase of ν_1 over time, when ignoring an outlier from literature (Kurtz et al. 1994). However, the new data from TESS and BRITE contradict clearly this simple view and call for a different explanation.

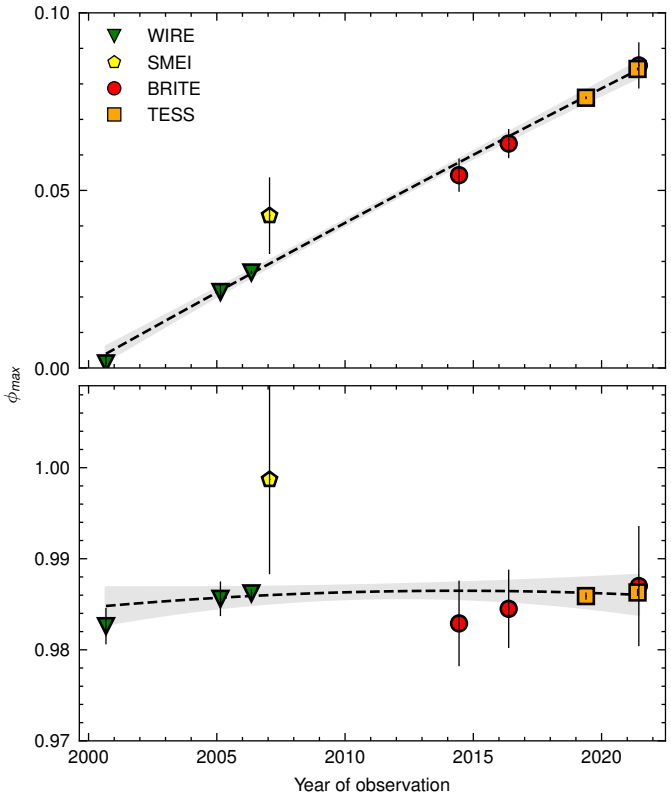

Fig. 6. Rotation phase of the light maxima with reference to our initial guess of P_{rot} (top) and the finally adopted value (bottom). Dashed lines indicate parabolic fits with the grey-shaded area giving the uncertainties.

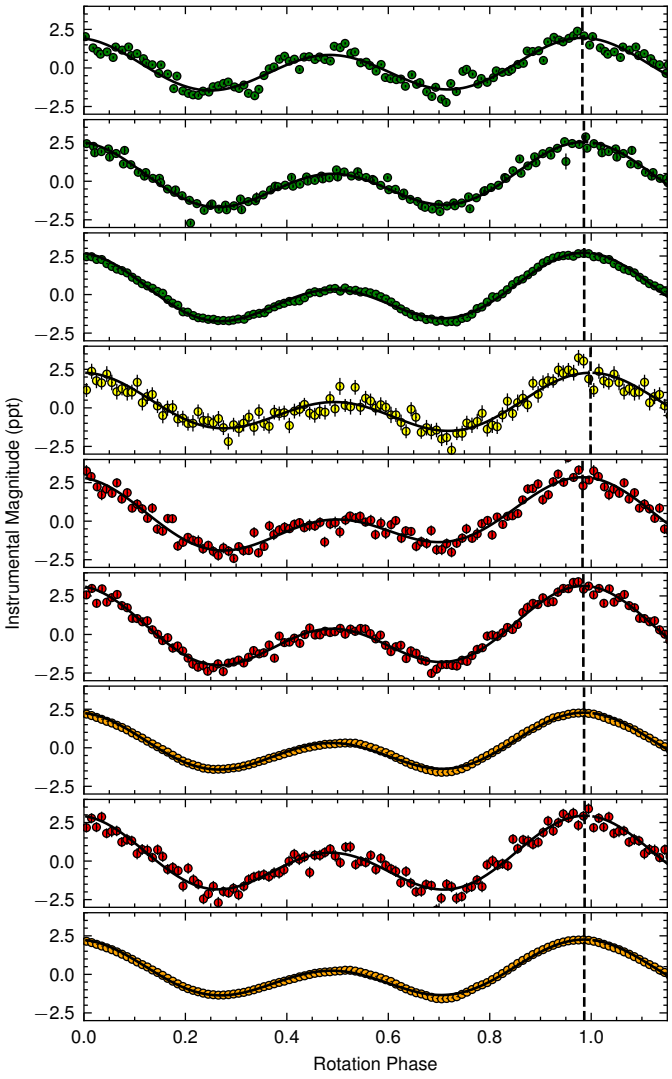

Fig. 7. Heavily binned light curves of α Cir folded with the finally adopted rotation period sorted by their observing epoch. Solid lines correspond to fits with Eq. 1 and the vertical dashed lines indicate the measured phase of the light maxima. The data sets are sorted by their observing year and correspond from top to bottom to the WIRE 2000, 2005, and 2006 data, SMEI, BRITE 2014 and 2016 data, TESS 2019, BRITE 2021, and the TESS 2021 data.

In Section 4 we argue that the main component of the already known visual binary system actually is a close binary. If we would see this system edge-on we could estimate from Fig. 4 that an eclipse should have been visible some when between August 2019 and January 2020 (i.e. $T + P$ from Tab. 4) during the last periastron of the system. Unfortunately this is at least one months after the TESS 2019 observations ended so that we cannot make any statement about an eclipsing system. It is, however, plausible to assume that the binary orbital axis is orientated roughly parallel to α Cir$_A$'s rotation axis, which can be estimated from the stars radius, the projected rotational velocity value and the rotation period.

Bruntt et al. (2008) determined the radius of α Cir from interferometric measurements to $1.97 \pm 0.07\,R_\odot$, which gives an equatorial rotation velocity of 22.2 ± 0.7 km/s for the about 4.48 d rotation period. Since $v \sin i = 14 \pm 1$ km/s (Reiners & Schmitt 2003), $\sin i$ results in 0.63 ± 0.05.

According to Fig. 5, the companion mass would then range somewhere between 0.4 and $1.6\,M_\odot$. The high mass end of this range basically can be ruled out as it would make the two stars comparable in brightness (given the companion is not a neutron star) and the actual luminosity of α Cir$_A$ would decrease to about $5\,L_\odot$, which shifts the star below the zero-age main-sequence, considering the measured surface temperature. It is more plausible that the companion is a low-mass star, contributing only a small fraction to the total luminosity. A $0.4\,M_\odot$ main-sequence star has a luminosity of about $0.03\,L_\odot$ and therefore covers only about 0.3% of the systems total luminosity of about $10.5\,L_\odot$. The spectral signature of this supposed companion has – to our knowledge – not yet been found, not even in high signal-to-noise spectroscopic measurements.

In Section 5 we demonstrate that the rotation phases of maximum light in the individual spot-modulated timeseries of α Cir$_A$ can be used to improve the rotation period of α Cir$_A$ and, indeed, the final value of $P_{rot} = 4.479290 \pm 0.000002$ d, which is consistent with the value determined by Weiss et al. (2020), but ten times more accurate. In Fig. 7 we show heavily binned versions of the various light curves, folded with the final rotation period along with the fits to measure the phase of maximum light.

7. Conclusion

α Cir has now been observed with improving accuracy from ground and space over more than 40 years, using spectrographs and photometers. The rotation period, e.g., could be determined with an accuracy of ±0.4ppm, which consequently represents

one of the best known stellar rotation periods. Furthermore, α Cir has the richest frequency spectrum observed for any roAp stars, which promises spectacular insights about the structure and evolution of this group of peculiar stars.

In fact, the dominant pulsation period, ν_1, changes with time, but unexpectedly, the plausible first explanation, evolutionary effects, proved to be wrong. Instead we propose the existence of a close companion.

Obviously, new problems appeared due to higher precision of the data. The richness of the frequency spectrum, e.g., is foiled by phenomena not yet explained by theory, like the curvature of a dipole mode sequence, or an amplitude excess of rotational side-lobes, or yet not understood amplitude changes.

We conclude that α Cir needs to remain on high-level observing programs, including attempts to confirm the close companion. Also a focus on modelling of the internal structure of α Cir, considering in particular the effects of a magnetic field on the pulsation spectrum, is demanded.

Acknowledgements. This paper includes data collected by the TESS mission, which are publicly available from the Mikulski Archive for Space Telescopes (MAST). Funding for the TESS mission is provided by NASA's Science Mission directorate. Funding for the TESS Asteroseismic Science Operations Centre is provided by the Danish National Research Foundation (Grant agreement no.: DNRF106), ESA PRODEX (PEA 4000119301) and Stellar Astrophysics Centre (SAC) at Aarhus University. We thank the TESS team and staff and TASC/TASOC for their support of the present work. Furthermore, this paper is based on data collected by the BRITE Constellation satellite mission, designed, built, launched, operated and supported by the Austrian Research Promotion Agency (FFG), the University of Vienna, the Technical University of Graz, the Canadian Space Agency (CSA), the University of Toronto Institute for Aerospace Studies (UTIAS), the Foundation for Polish Science & Technology (FNiTP MNiSW), and National Science Centre (NCN).

References

Aerts, C. 2021, Reviews of Modern Physics, 93, 015001
Baldry, I. K., Bedding, T. R., Viskum, M., Kjeldsen, H., & Frandsen, S. 1998, MNRAS, 295, 33
Breger, M. & Pamyatnykh, A. A. 1998, A&A, 332, 958
Bruntt, H., Kurtz, D. W., Cunha, M. S., et al. 2009, MNRAS, 396, 1189
Bruntt, H., North, J. R., Cunha, M., et al. 2008, MNRAS, 386, 2039
Buchner, J. 2016, Statistics and Computing, 26, 383
Buzasi, D. 2002, in Astronomical Society of the Pacific Conference Series, Vol. 259, IAU Colloq. 185: Radial and Nonradial Pulsationsn as Probes of Stellar Physics, ed. C. Aerts, T. R. Bedding, & J. Christensen-Dalsgaard, 616
Cunha, M. S. 2006, MNRAS, 365, 153
Feroz, F., Hobson, M. P., & Bridges, M. 2009, MNRAS, 398, 1601
Gough, D. 1985, Nature, 314, 14
Holdsworth, D. L., Cunha, M. S., Kurtz, D. W., et al. 2021, MNRAS, 506, 1073
Jackson, B. V., Buffington, A., Hick, P. P., et al. 2004, Sol. Phys., 225, 177
Jeffreys, H. 1998, Theory of probability, Oxford Classic Texts in the Physical Sciences (New York: The Clarendon Press Oxford University Press), xii+459, reprint of the 1983 edition
Jenkins, J. M., Twicken, J. D., McCauliff, S., et al. 2016, in Society of Photo-Optical Instrumentation Engineers (SPIE) Conference Series, Vol. 9913, Software and Cyberinfrastructure for Astronomy IV, ed. G. Chiozzi & J. C. Guzman, 99133E
Kallinger, T. & Weiss, W. W. 2017, in Second BRITE-Constellation Science Conference: Small Satellites - Big Science, ed. K. Zwintz & E. Poretti, Vol. 5, 113–119
Kallinger, T., Weiss, W. W., Beck, P. G., et al. 2017, A&A, 603, A13
Kurtz, D. W. 1982, MNRAS, 200, 807
Kurtz, D. W., Allen, S., & Cropper, M. S. 1981, Information Bulletin on Variable Stars, 2033, 1
Kurtz, D. W. & Balona, L. A. 1984, MNRAS, 210, 779
Kurtz, D. W., Sullivan, D. J., Martinez, P., & Tripe, P. 1994, MNRAS, 270, 674
Lenz, P. & Breger, M. 2005, Communications in Asteroseismology, 146, 53
Mathys, G. 2017, A&A, 601, A14
Mkrtichian, D. E. & Hatzes, A. P. 2013, in Astronomical Society of the Pacific Conference Series, Vol. 479, Progress in Physics of the Sun and Stars: A New Era in Helio- and Asteroseismology, ed. H. Shibahashi & A. E. Lynas-Gray, 115
Monier, R. 2020, Research Notes of the American Astronomical Society, 4, 160
Pablo, H., Whittaker, G. N., Popowicz, A., et al. 2016, PASP, 128, 125001
Popowicz, A., Pigulski, A., Bernacki, K., et al. 2017, A&A, 605, A26
Reiners, A. & Schmitt, J. H. M. M. 2003, A&A, 412, 813
Ricker, G. R., Winn, J. N., Vanderspek, R., et al. 2015, Journal of Astronomical Telescopes, Instruments, and Systems, 1, 014003
Ryabchikova, T., Sachkov, M., Kochukhov, O., & Lyashko, D. 2007, A&A, 473, 907
Schneider, H. & Weiss, W. W. 1983, Information Bulletin on Variable Stars, 2306, 1
Schneider, H. & Weiss, W. W. 1989, A&A, 210, 147
Sinachopoulos, D. 1989, A&AS, 81, 103
Tassoul, M. 1980, ApJS, 43, 469
Trifonov, T., Tal-Or, L., Zechmeister, M., et al. 2020, VizieR Online Data Catalog, J/A+A/636/A74
Weiss, W. W., Fröhlich, H. E., Kallinger, T., et al. 2020, A&A, 642, A64
Weiss, W. W., Fröhlich, H. E., Pigulski, A., et al. 2016, A&A, 588, A54
Weiss, W. W. & Schneider, H. 1984, A&A, 135, 148